Desalination and Water Treatment
www.deswater.com

doi: 10.5004/dwt.2023.29177

285 (2023) 156–166
February

Preparation of CNTs/silica composite aerogels beads by a water-in-oil emulsion method and a study of their application in the removal of toluene from an aqueous mixture

Mingbo Jiang[a,*], Chenggong Ju[b], Zhitao Du[a], Jing Liu[a], Xiao Peng[b], Yan Wu[b,*]

[a]*Beijing Institute of Applied Meteorology, No. 8 Minzuyuan Road, Chaoyang District, Beijing, China, Tel.: +(86) 1055482552/ +(86)18910802257; emails: qxjlcs@163.com (M. Jiang), 527239365@qq.com (Z. Du), 454684189@qq.com (J. Liu)*
[b]*College of Chemical Engineering and Materials Science, Tianjin University of Science and Technology, No. 29 13th Avenue, Economic and Technologic Development Zone, Tianjin, China, Tel.: +(86) 022-60601457; Fax: +(86) 022-60602845; emails: wuyan_tust@163.com (Y. Wu), juchenggong@tust.edu.cn (C. Ju), pengxiao@tust.edu.cn (X. Peng)*

Received 15 May 2022; Accepted 29 November 2022

ABSTRACT

Utilizing silica sol as precursor and carbon nanotubes (CNTs) as additives, the CNTs/silica composite aerogels beads (CS-CABs) with different CNTs content were synthesized by a water-in-oil emulsion method combining sol–gel process. The effects of content of CNTs on the macro- and micro-morphology, even pore structure of CS-CABs were investigated by scanning electron microscopy and N_2 adsorption–desorption measurement. The results reveal that CNTs have great influence on their morphology and pore structure characteristics. When the addition amount of CNTs is 0.4%, CS-CABs (labeled as 0.4% CS-CABs below) yield the best overall performance of removing toluene in aqueous bodies, and its corresponding values of surface area, pore diameter and pore volume are 321 m^2/g, 38.56 nm and 1.44 cm^3/g, respectively. Furthermore, the 0.4% CS-CABs was characterized by Fourier-transform infrared spectroscopy, X-ray powder diffraction and contact angle analysis, and the mechanism of isotherm and adsorption kinetics were also studied. The maximum saturated adsorption capacity of toluene under 293 K is as high as 214 mg/g, which is about 1.2 and 1.4 times to SiO_2 aerogels beads and CNTs. Freundlich model and quasi-first-order kinetic adsorption model fit the adsorption process well, and it is proved that the adsorption process is dominated by physical adsorption.

Keywords: Silica aerogels; Carbon nanotubes; Aerogels beads; Adsorption; Mesoporous

1. Introduction

Aerogels is currently one of the most highly porous nanostructured materials [1]. Silica aerogels consists of tangled, fractal-like chains of spherical clusters of SiO_2 of 3–4 nm in diameter, and the chains form a solid structure surrounding air-filled pores whose average diameter is about 20 nm [2,3], which endows it with low density (3 kg/m^3), high porosity (99%), small pore size (1–100 nm), open mesoporous structure and high surface area [4–7]. Due to its excellent properties, silica aerogels have great potential applications in the fields of science and technology, such as drug delivery carriers, thermal insulation materials, supports for catalysts, and adsorbents for organics [5,8].

Toluene, an important chemical raw material [2,9], is widely used in industry as a diluent for paints, coatings or adhesives [9,10]. However, water pollution caused by toluene emissions has already become a concern of environmental issues. Toluene leaking into the aquatic ecosystem will cause water pollution and death of aquatic organisms, while

* Corresponding authors.

endangering human health and safety [9–12]. Therefore, the strategy of effective removal of toluene or other BTEX (benzene, ethylbenzene, p-xylene) from water environment is necessary. Current technologies for BTEX removal from water include biological treatment [13,14], chemical treatment, and adsorption methods by various sorbents [2,15]. Among these three processes, adsorption is widely applied for its flexibility, low cost and low energy consumption [2,6,8,15]. Silica aerogels is one of the most commonly used hydrophobic and mesoporous adsorbents [16]. Compared with porous carbon materials that is dominated by micropores [17,18], silica aerogels have better selective adsorption properties with higher saturated adsorption amount, due to its mesoporous nature [16,17,19,20]. In addition, silica aerogels can be chemically modified to improve the surficial hydrophobicity, thus to achieve selective adsorption of target specific compounds, and thus further enhance the adsorption efficiency. Kumagai et al. [21] found that silica aerogels modified with methyltrimethoxysilane (MTMS) or trimethylethoxysilane exhibited high adsorption capacities for toxic organic compounds from water. Wang et al. [22] showed that hydrophobic silica aerogels exhibited strong adsorption capacity on slightly soluble organic.

Carbon nanotubes (CNTs) [23,24], with their tubular one-dimensional (1D) structure, are stable in chemistry, and it shows outstanding properties for the application in electricity, mechanics, especially in adsorption. And it has been employed to remove toluene and other organic pollutants from aqueous bodies in previous reports [10,25]. The excellent adsorption properties of CNTs for toluene is attributed to the large specific surface area and the π–π interaction [26,27]. In addition, CNTs are widely used in the fabrication of composite materials, in order to improve their mechanical strength. Karim et al. [28] have successfully compounded silica aerogels with functionalized multi-walled carbon nanotubes (MWCNTs) via a sol–gel process, which improved the mechanical properties of silica aerogels. Liu et al. [29] have prepared reinforced silica aerogels with tungsten disulfide nanotubes, and explored the best doping amount, and the results showed that the addition of 0.1 wt.% of CNTs to the brittle porous matrix can effectively increases the toughness. Menshutina et al. [30] have prepared silica aerogels monoliths embedded with different amount MWCNTs. However, there are few studies on the adsorption properties of CNTs/SiO_2 composite aerogels. Based on the excellent adsorption properties of CNTs and silica aerogels, silica aerogels combined with CNTs can take a combined advantage to obtain more excellent adsorption characteristics. Moreover, in the current reports, silica aerogels and CNTs are mainly composed of bulk or powder form, which would limit their practical application in adsorption. Bulk materials are inconvenient to fill, and its internal adsorption efficiency is generally unsatisfactory [1,31]. Though aerogels powder has the characteristics of efficient and rapid adsorption, the cost of adsorbents is relative high, furthermore specific resistance of filtration process is large. And more importantly, it is difficult to maintain water quality [32,33], because it is extremely challenging to completely remove aerogels powder from water. In order to solve these problems, the silica composite aerogels could be shaped into beads [21,34–36], which can both ensure the adsorption efficiency and speed at the same time. In addition, silica aerogels beads have smaller flow resistance, lower friction coefficient, good fluidity and uniform force, which made it conducive to the developing computational model. Conventional methods for preparing silica aerogels beads include inkjet method [37], ball drop method [38,39] and emulsion method [33,35,36,40–44]. Among which, although that the silica aerogels beads prepared by the inkjet method or the ball drop method possess good skeleton stability and adapt to the ambient drying technique, the prepared aerogels beads are usually large and uneven in size, which is not conducive to filling and modeling in practical adsorption applications. The emulsion method is mainly water-in-oil (W/O) emulsion method. Using water glass as the source of silicon, through dropwise addition of the silica sol into *n*-hexane to form wet gel beads, Zong et al. [40] prepared the silica aerogels beads with a diameter of about 1 mm after drying under ambient pressure. Sarawade et al. [36] have synthesized spherical aerogels micro particles under supercritical drying conditions by in situ W/O emulsion polymerization, and the synthesized microspheres have large specific surface area and uniform particle size distribution. Yu et al. [33] synthesized silica aerogels beads through a two-step acid-base sol–gel reaction in W/O emulsions via supercritical drying, and the influence of experimental parameters on the balling was discussed. Sing [44] have synthesized micrometer-sized (4–20 μm) silica aerogel microspheres at ambient pressure through emulsion method combined with solvent replacement and surface modification, the effect of the processing conditions on the size and morphology was discussed. The microspheres prepared by the above emulsion methods all have regular spherical shape and uniform size, which provides important theoretical support for the preparation of silica aerogels composite beads.

In this study, silica sol was chosen as silicon precursors, CNTs/SiO_2 aerogels composite beads (CS-CABs) with different CNTs contents were prepared by W/O emulsion method, combined with sol–gel process under conventional drying conditions. Effects of CNTs on the particle size, morphology and inner porous structure of CS-CABs were also investigated. The adsorption properties of CS-CABs to toluene in aqueous were performed, and the corresponding isotherm and adsorption kinetics were also studied. To the best of our knowledge, this is the first time to report the preparation of CNTs/silica composite aerogels beads and application in the adsorption of toluene in aqueous environment.

2. Experiments

2.1. Chemicals

Carbon nanotubes (CNTs) (97%) were purchased from Shenzhen Nanotech Port Co., Ltd. Ammonia solution (28 wt.%, AR), ethanol (95 wt.%, AR), sulfuric acid (AR) and the nitric acid (AR) were obtained from Sinopharm. Silica sol (JN-30) was supplied by Grade Group, Qingdao. n-heptane (AR), n-butyl alcohol (AR), Span 80 (CP) and

Tween 85 (CP) were purchased from Fengchuan Group. All chemicals were used as received without further purification.

2.2. Preparation of oxidized carbon nanotubes (CNTs-COOH)

In order to enhance the polarity of CNTs, thus increasing their dispersibility in water, and realize the purpose of purification, CNTs were firstly oxidized by the concentrated sulfuric acid and nitric acid before use. Typically, 1 g of CNTs were dispersed into a mixed solution that consists of 90 mL of H_2SO_4 and 30 mL of HNO_3 under ultrasonication for 30 min, followed by reflux in a flask at 60°C–65°C for 4 h. After washing with deionized water and other chemical reagents, followed by drying at 60°C for 12 h, the pretreated CNTs-COOH samples were obtained.

2.3. Preparation of CNTs/silica composite aerogels bead

The CS-CABs with different CNTs doping content were synthesized by a W/O emulsion method in a sol–gel process. The scheme of the synthetic process is shown in Fig. 1. Typically, CNTs were dispersed in ethanol under ultrasonication for 30 min to obtain the CNTs dispersion of different mass ratio (0%, 0.2%, 0.4%, 0.6%, 0.8%, and 1.0%). Silica sol was firstly mixed with 1 mL of nitric acid solution (5 wt.%), and then poured into the aforementioned CNTs dispersion to form the alcohol sol phase (dispersed phase). 0.034 g of Span 80 and 0.0034 g of Tween 85 were dissolved in 25 mL of n-heptane solution under continuous stirring for 30 min, and then 2.5 mL of n-butyl alcohol was added to form an micro emulsion. The alcohol sol (dispersed phase) was added into the micro emulsion dropwise whilst stirring to form the W/O emulsion, and the pH was adjusted to 7.0 with ammonia solution ($VN_{H_3H_2O}$:V_{H_2O} = 1:10). The obtained silica wet gel beads were washed repeatedly with acetone and collected by centrifugation, followed by aging at 60°C in a tetraethoxysilane (TEOS)/EtOH (V_{TEOS}:V_{EtOH} = 1:3) bath for 12 h. In order to obtain hydrophobic silica aerogels beads, the as prepared silica wet gel beads were modified in an 10% trimethylchlorosilane (TMCS)/n-hexane solution for 6 h at 60°C. Next, the product was dried in vacuum at 30°C for 6 h to acquire the dry CNTs-COOH/silica aerogels beads (COS-CAMs), then it was further heated in a horizontally tubular furnace under N_2 atmosphere at 300°C for 3 h.

Here, the W/O emulsion templating method was used to prepare the silica aerogel beads. Another similar emulsion templating method based on HIPE (high internal phase emulsion) is also an efficient way to obtain highly porous polymeric materials called poly-HIPE materials, and has been applied to prepare the degradable material for tissue engineering [45]. The difference of the two methods is that for the HIPE templating method, the external phase was solidified to form the bulk template, and the internal phase (droplets) was used to form the inner pores. While for the method we applied, the silica beads just formed inside the internal phase (droplets), and the pores formation arose from the volatilization of the aqueous phase. And the emulsion formation was for the separation of the droplets, which finally turned into the silica beads.

2.4. Characterizations

The density of the obtained CS-CABs was calculated based on their mass-to-volume ratios. The macroscopic morphology of CS-CABs was characterized by optical microscopy (BK-POL, OPTEC, China) and the surface physical morphology was further examined by scanning electron microscopy (SEM) (SU-1510, Hitachi, Japan) at 0.3–3 kV. N_2 adsorption–desorption isotherm was measured on Autosorb-iQ, and specific surface area was determined

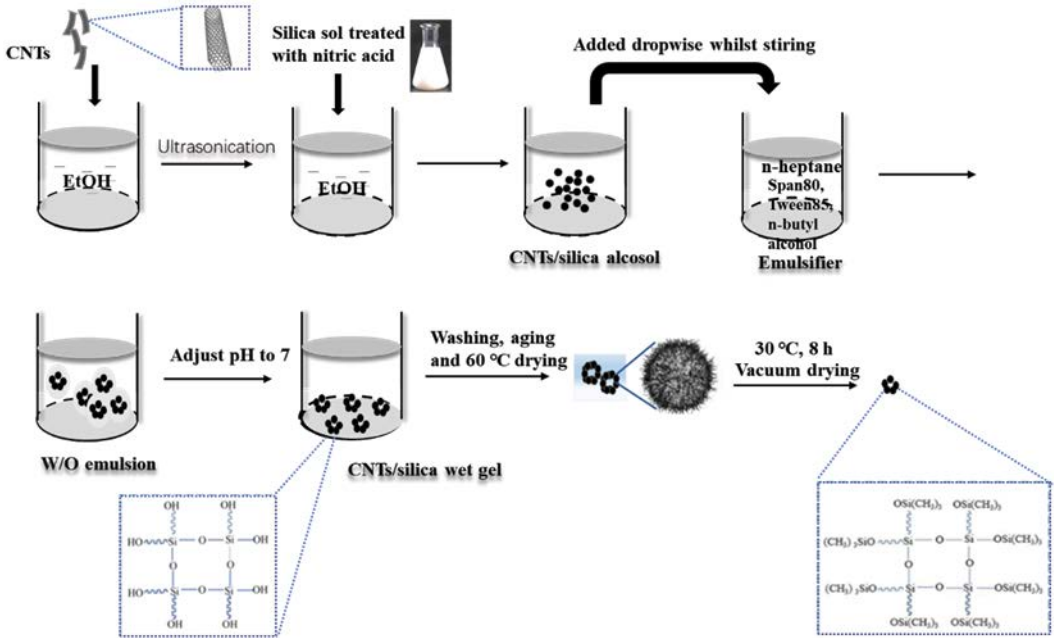

Fig. 1. Scheme of synthetic process of CS-CABs.

according to the Brunauer–Emmett–Teller (BET) method in the relative pressure (P/P_0) range of 0.0001–0.9990, and the pore-size distribution was calculated using the Barrett–Joyner–Halenda (BJH) model. The surface functional groups were detected by a Fourier-transform infrared spectroscopy (FT-IR) spectrometer (Tensor 27, Bruker, Germany) equipped with a KBr beam splitter (KBr, FT-IR grade). The crystal structure of the CS-CABs was characterized using X-ray powder diffraction (XRD) (6100, Shimadzu, Japan) diffractometer using CuK/radiation (40 kV, 100 mA, k = 1.5406 Å), wide angles were obtained in the 2θ range from 10 to 80, employing a scanning rate of 2°/min^{-1}. Surficial hydrophobicity of CS-CABs was determined by contact angle (θ) measurements, which performed using a contact angle meter (DSA30, Kruss, Germany), and the samples were measured after pressed into tablet. The particle size distribution of CS-CABs was measured by dynamic laser particle sizer (MS2000, Malvern, Britain).

2.5. Adsorption experiments

A toluene adsorption measurement was performed as follows: 0.02 g of adsorbents (SiO_2 aerogels beads, CNTs or 0.4% CS-CABs) were added into a 250 mL conical flasks, respectively, and then 100 mL of solutions with toluene content in the range of 20–100 mg/L were added. The pH was adjusted to 7 by 0.1 mol/L of NaOH. After stirring until reaching adsorption equilibrium at 293, 313 or 333 K, 10 mL of solution was withdrawn and centrifuging at 6,000 rpm for 20 min. The supernatant was drawn as sample, and the absorbance of toluene (261 nm) solution was measured by UV-Vis spectrophotometer (UV-1800, China, Mapada). The saturated adsorption capacity of toluene was calculated according to the standard curve of toluene.

$$q_t = \frac{(C_0 - C)V}{m} \tag{1}$$

where C_o is the initial concentration (mg/L) and C is the equilibrium concentrations (mg/L). V is the volume of the added solution (L), and m is the mass of the adsorbent used (g), q_t is the amount of adsorbate (mg/g).

The equilibrium data of toluene aqueous solution adsorption on each samples at different temperatures were fitted. Langmuir and Freundlich isotherms are the two most commonly used models for liquid–solid adsorption systems. Langmuir adsorption isotherms are mainly based on the following two ideal assumptions: the adsorption process between adsorbate and adsorbent is similar to reversible chemical reaction, and adsorption is mainly monolayer adsorption; the adsorption heat is independent of the surface coverage and there is no interaction between the adsorbed molecules. The expression is as follows [39]:

$$\frac{C_e}{q_e} = \frac{1}{q_b} + \frac{C_e}{Q} \tag{2}$$

where C_e is the adsorbate concentration (mg/L) at equilibrium, q_e (mg/g) is the solid-phase adsorbate concentration at equilibrium, q_b is the Langmuir adsorption constant, and Q is the maximum adsorption capacity of adsorbent (mg/g).

The Freundlich isothermal adsorption model is based on assumption that adsorption occurs at specific adsorption sites or at surface support sites with variable adsorption capacity. The model assumes that strong bonds and sites are occupied first and that the bonding strength decreases as the surface sites are occupied. The expression is as follows [39]:

$$\ln q_e = \ln K_F + \frac{1}{n}\ln C_e \tag{3}$$

where C_e is the concentration (mg/L) at equilibrium of the adsorbate, q_e (mg/g) is the equilibrium adsorption capacity of the adsorbent, n is the exponent Freundlich adsorption constant, K_F is the proportionality Freundlich adsorption constant.

Adsorption kinetics [46] study was performed to investigate the relationship between adsorption rate and activation energy. It mainly describes the change of adsorption amount of pollutants on adsorbent/water phase over time. Here, pseudo-first-order kinetic and pseudo-second-order kinetics model were used as classical references.

Pseudo-first-order and pseudo-second-order kinetic expressions are shown as follows:

$$Q_t = Q_e\left(1 - e^{-kt}\right) \tag{4}$$

$$\frac{dQ_t}{dt} = K\left(Q_s - Q_t\right) \tag{5}$$

where Q_t is the adsorption capacity of CS-CABs at the adsorption time t, Q_s and Q_e are the saturated adsorption capacity, and K is the adsorption rate constant of the model, which characterizes the adsorption rate of the solute.

3. Results and discussion

3.1. Effect of CNTs addition on CS-CABs performance

The trends of density of CS-CABs with different CNTs content are illustrated in Fig. 2. The density of the CS-CABs is 289 kg/m^3 without CNTs doping. It is obvious that density of the synthesized CS-CABs increased with the increase of dosing amount of CNTs. When the amount of CNTs is as high as 1%, the density of the CS-CABs is merely 410 kg/m^3, thus it could be still regarded as a light material.

It could be seen from Fig. 3 that the particle size of the CS-CABs was also increasing with the addition of CNTs, and the photographs taken by optical microscope of the CS-CABs corresponding to different additive amount of CNTs was embedded in Fig. 3. It demonstrates that the doping amount of CNTs has great influence on the morphology of CS-CABs. When the CNTs content is 0.2%–0.8%, the particle size distribution of the CS-CABs is uniform and their sphericity is well enough. However, when the addition of CNTs reached up to 1%, the shape of CS-CABs is unable to maintain well spherical, due to the probable aggregation of CNTs.

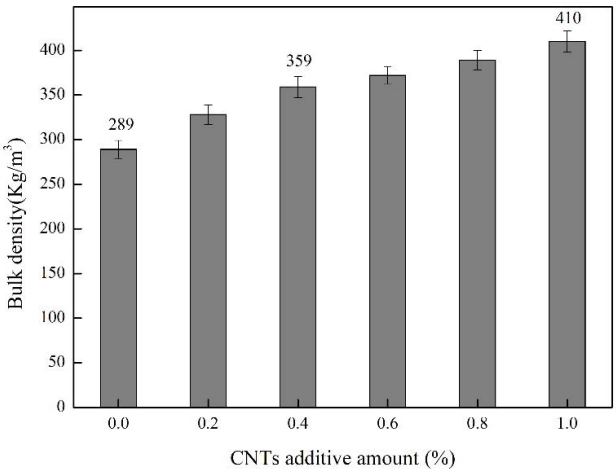

Fig. 2. Density of CS-CABs with different CNTs additions.

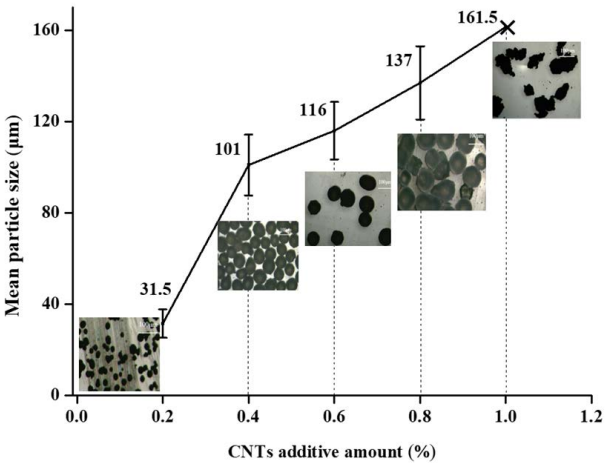

Fig. 3. Particle size of CS-CABs with different CNTs additions.

Moreover, the influence of the addition of CNTs on the particle size of CS-CABs is further analyzed. When silica aerogels dried under atmospheric environment, the change of surface tension would lead a collapse or shrinkage of three-dimensional porous structure. However, as the content of CNTs was in the range of 0.4%–0.8%, the added CNTs could effectively prevent CS-CABs from collapse, and thus the particle size of the prepared bead would grow along with the increase of CNTs content.

The data of specific surface area, pore volume, pore diameter of CS-CABs with different CNTs doped are listed in Table 1. Among which, it could be seen that all these three parameters of un-doped silica aerogels beads are the smallest. Compared with the un-doped ones, even a relative low CNTs content can effectively increase the specific surface area, pore volume and the pore size of the composite aerogels beads. It could demonstrate that CNTs can support the three-dimensional porous structure of aerogels beads, due to its excellent mechanical properties, and it is further beneficial to the enhancement of the adsorption properties as a result. However, unlike the change trend of particle size,

Table 1
BET surface area, pore volume, pore size, and porosity of CS-CABs

Doping amount (%)	Specific surface area (m^2/g)	Pore volume (cm^3/g)	Pore diameter (nm)
0	286	1.12	16.24
0.2	298	1.25	19.52
0.4	321	1.44	38.56
0.6	316	1.41	29.96
0.8	305	1.37	22.97
1.0	299	1.32	21.18

values of three aforementioned parameters first ascended and then descended with the addition of CNTs, with a critical content of CNTs of 0.4%. The possible reason is that agglomeration of extra CNTs in the inner porous structure of aerogels beads might block the pores, and result in the decrease of specific surface area, pore volume, and pore diameter. Even so, the specific surface area of the composite is still larger than that of the silica aerogels beads without CNTs. Data in Table 1 indicates that under the presence of the suitable amount of CNTs (especially 0.4%), the value of surface area, pore diameter and pore volume of the beads could reach 321 m^2/g, 38.56 nm and 1.44 cm^3/g, respectively.

The N_2 adsorption and desorption isotherms of 0.4% CS-CABs at 77 K and the corresponding pore-size distributions obtained by the BJH method are shown in Fig. 4. As shown in Fig. 4a, according to the IUPAC classification [46], adsorption isotherm curves for 0.4% CS-CABs could be considered as type IV, which corresponded to the characteristic features of mesoporous materials [47]. Furthermore, the 0.4% CS-CABs showed similar isotherms (H1 type) and were comparable to supercritical/ambient pressure dried silica aerogels [39], indicating it possessed cylindrical pores [47]. And the larger the hysteresis loops, the more the cylinder pores in the aerogels network [39]. The N_2 adsorption rate in the micropores increases slowly at low pressures ($P/P_0 < 0.1$), but increases obviously for mesopores at higher P/P_0 (0.1–0.8). Thus the N_2 adsorption result indicates the existence of a large number of mesopores inside the aerogel. The rapid rise of isotherm at high P/P_0 (0.8–1.0) reveals the presence of a few macropores (>50 nm). In conclusion, micro-, meso- and macropores all exist in the 0.4% CS-CABs, and the size distribution of the contained pores ranges from 4 nm to 117 nm, with a peak pore diameter appearing at 47 nm (Fig. 4b). Thus, the 0.4% CS-CABs have well-developed porous structures, and the mesopores is dominant.

3.2. Structural characterization of 0.4% CS-CABs

SEM was utilized to reveal the skeleton structure of beads. It could be seen from the Fig. 5b that compared with un-doped silica aerogels (Fig. 5a), the CNTs uniformly distributed on the surface of 0.4% CS-CABs. The CNTs supported the inner porous structure of silica aerogels beads, and the 0.4% CS-CABs exhibit loose and porous appearance (Fig. 5b). The model diagram of composite aerogels beads

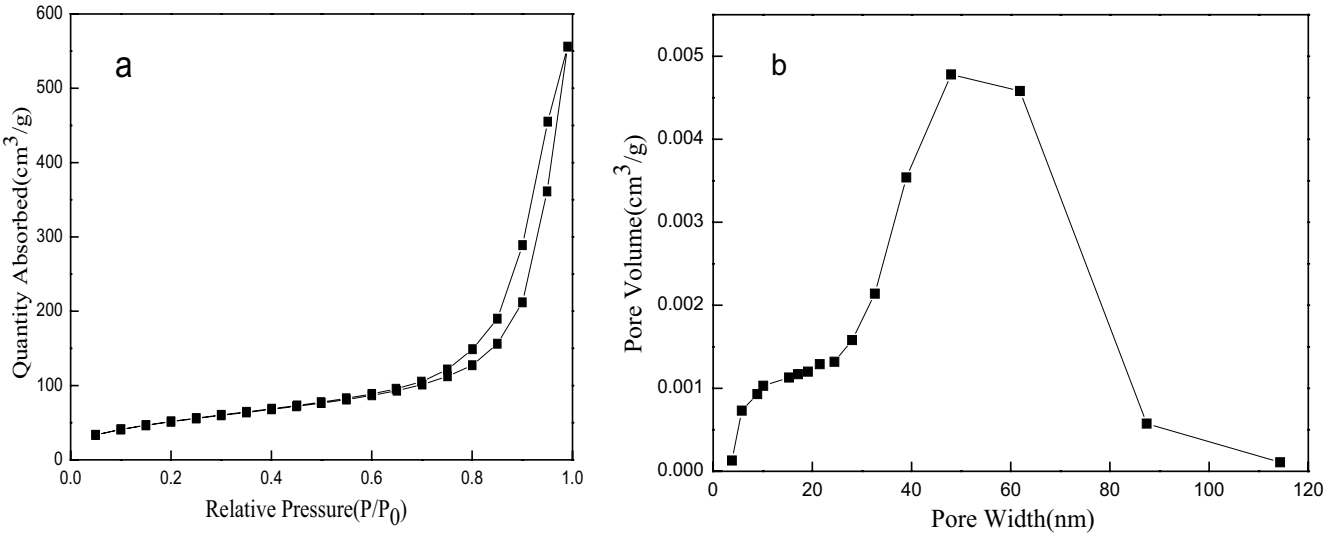

Fig. 4. Nitrogen adsorption/desorption isotherms (a) and BJH pore-size distribution (b) of 0.4% CS-CABs the microscopic model diagram.

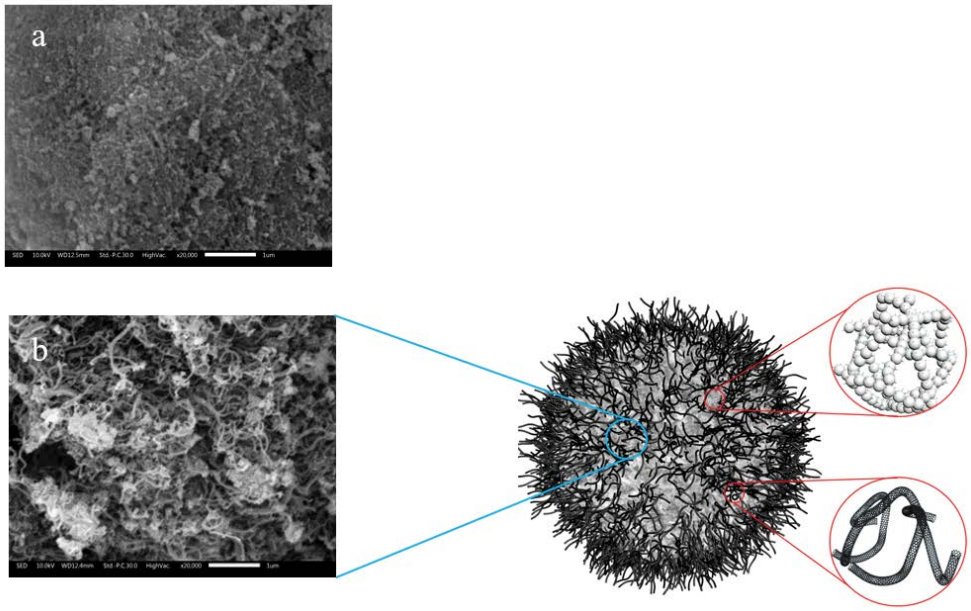

Fig. 5. Microstructure of silica aerogels beads and CS-ACMs.

is also shown in Fig. 5, the obtained aerogels are a three-dimensional bead with opening pores, consisting of tangled, fractal-like chains of spherical clusters of SiO_2. The CNTs distribute uniformly on the surface and inner channel of the composite. Compared with the similar poly-HIPE materials, which possess similar bulk density and porosity to 0.4% CS-CABs [45], the voids or pores inside the beads are smaller, which originates from the aforementioned fact that the voids are formed through the evaporation of aqueous part of the droplets, and has been confirmed by Fig. 5.

Fig. 6 shows the FT-IR spectra of modified 0.4% CS-CABs before and after heat-treated in N_2 at 300°C. The peaks at 1,074; 824 and 472 cm^{-1} correspond to the Si–O–Si bonds, which are the signature peaks of the silica network structure [40]. The peaks centered at 2,930~2,840 cm^{-1} assigned to terminal $–CH_3$ groups, which are attributed to surface modified by TMCS [40]. Moreover, $–CH_3$ groups did not decrease significantly in Fig. 6 after heat treatment, which demonstrated that 0.4% CS-CABs treated at 300°C can maintain its hydrophobic surficial nature. The strong peak of 3,430 cm^{-1} related to –OH, the oxygen-containing functional groups formed by strong acid oxidation of carbon nanotubes. After heat treatment at 300°C, the –OH oxygen-containing functional groups of the 0.4% CS-CABs significantly

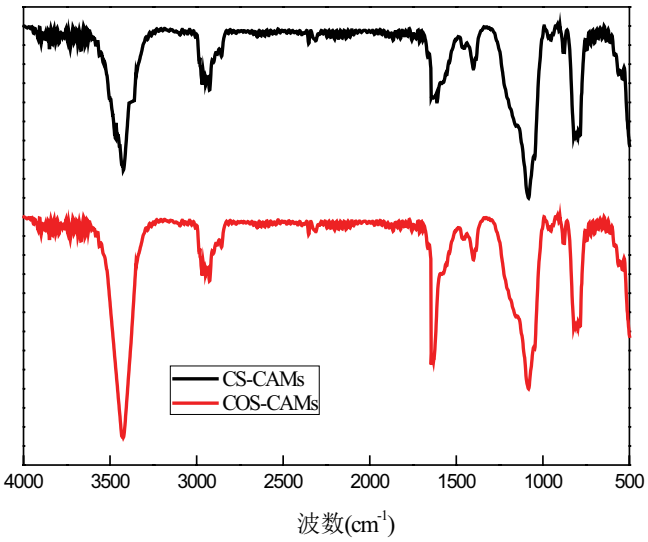

Fig. 6. Infrared analysis of COS-CAMs and CS-CABs.

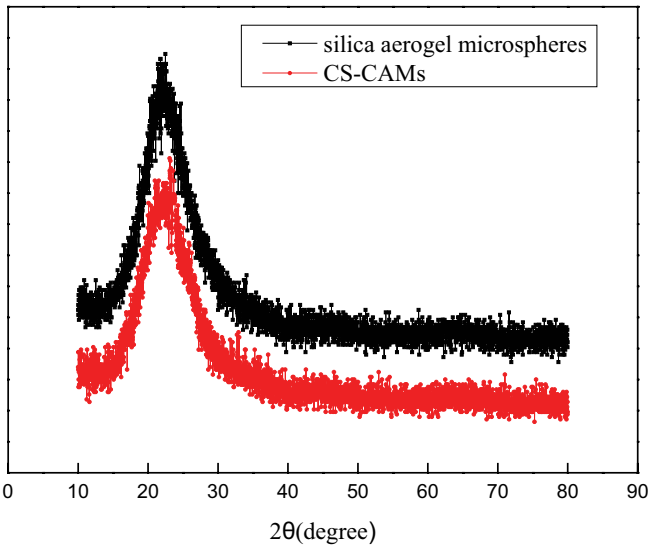

Fig. 7. XRD patterns of 0.4% CS-CAMs.

reduced, and the change indicates the reduction of CNTs-COOH. It explains the improvement of the hydrophobicity of the composite aerogels beads after heat-treatment, which is beneficial to toluene adsorption.

The X-ray diffraction (XRD) patterns of silica aerogels beads and 0.4% CS-CABs samples are presented in Fig. 7. The broad line centered at 18°–28° is attributed to the amorphous structure of the silica matrix. CNTs can be purified by oxidation [24], thus after oxidation by nitric acid and sulfuric acid, the XRD pattern of CNTs is similar to that of silica aerogels beads [26] without any heterozygous peaks [24]. Therefore, there is only a wider diffraction peak between 18°–28° in the 0.4% CS-CABs left after heat treatment.

Fig. 8 shows the particle size distribution curve of 0.4% CS-CABs. It can be seen that the composite aerogels beads mainly distributed at 60–120 μm, and reached the peak value at 86 μm. The results reveal that, when the content

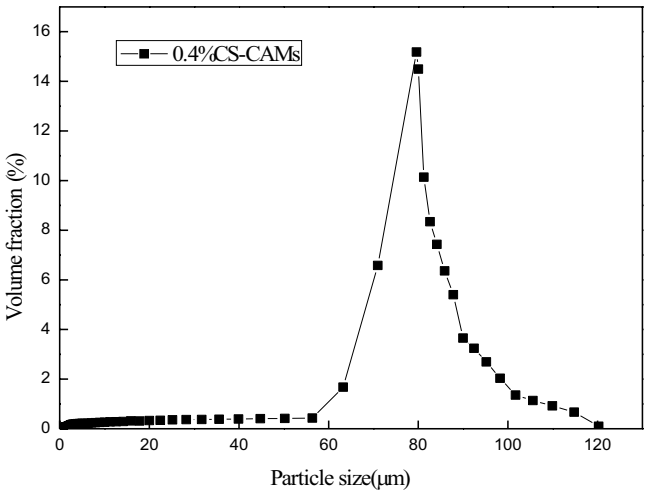

Fig. 8. Particle size distribution of 0.4% CS-CABs.

of CNTs is 0.4%, not only the spherical shape of CS-CABs can be maintained, but also the uniform particle size distribution can be obtained. Homogeneous beads would have smaller flow resistance, lower friction coefficient, better fluidity and more uniform load conditions, which made it conducive to the establishment of the calculation model [33–35].

Photography of contact angle of 0.4% CS-CABs are shown in Fig. 9. Hydrophobic silica aerogels exhibited strong adsorption capacity on slightly soluble organic compounds [6] due to the poor water solubility of toluene, and TMCS is used for its surface hydrophobic modification. The contact angle of 0.4% CS-CABs before and after modification increases from 60° to 132°, which transfers its surface nature from hydrophilicity to hydrophobicity. The main reason is that mass of the hydrophobic $–CH_3$ from TMCS replaces the native –OH of 0.4% CS-CABs surface. Hence, modified 0.4% CS-CABs seems easier to affinity and adsorb organic from water. Besides, the surface modification will reduce the surface tension and prevent the pore from collapse in the drying process.

3.3. Characterization of adsorption properties of 0.4% CS-CABs

Adsorption isotherm is important for describing the interaction of solutes and adsorbent [15]. Fig. 10 presents the adsorption isotherm of CNTs, silica aerogels beads and 0.4% CS-CABs in the toluene solution at different temperature (293, 313 and 333 K). From a study of toluene adsorption at different concentrations and temperatures, the maximum capacity of the composites was found to be 214 mg/g, which it is 1.2 and 1.4 times that of silica aerogels beads and CNTs, respectively. The optimum temperature was 293 K and the optimal composite composition was the aforementioned 0.4% CNT. Moreover, the adsorption capacity of adsorbent decreases with increasing temperature. The data of the adsorption capacity calculated from the residual toluene concentration were used to simulate the Langmuir and Freundlich isotherm separately. As is shown in Fig. 10, the experimental data are represented by solid symbols, the green solid line represents the data fitted by

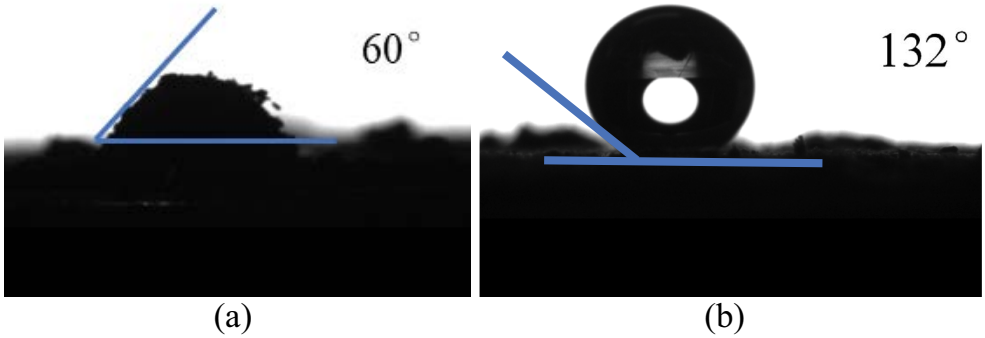

Fig. 9. Contact angle of (a) unmodified and (b) modified CS-CABs.

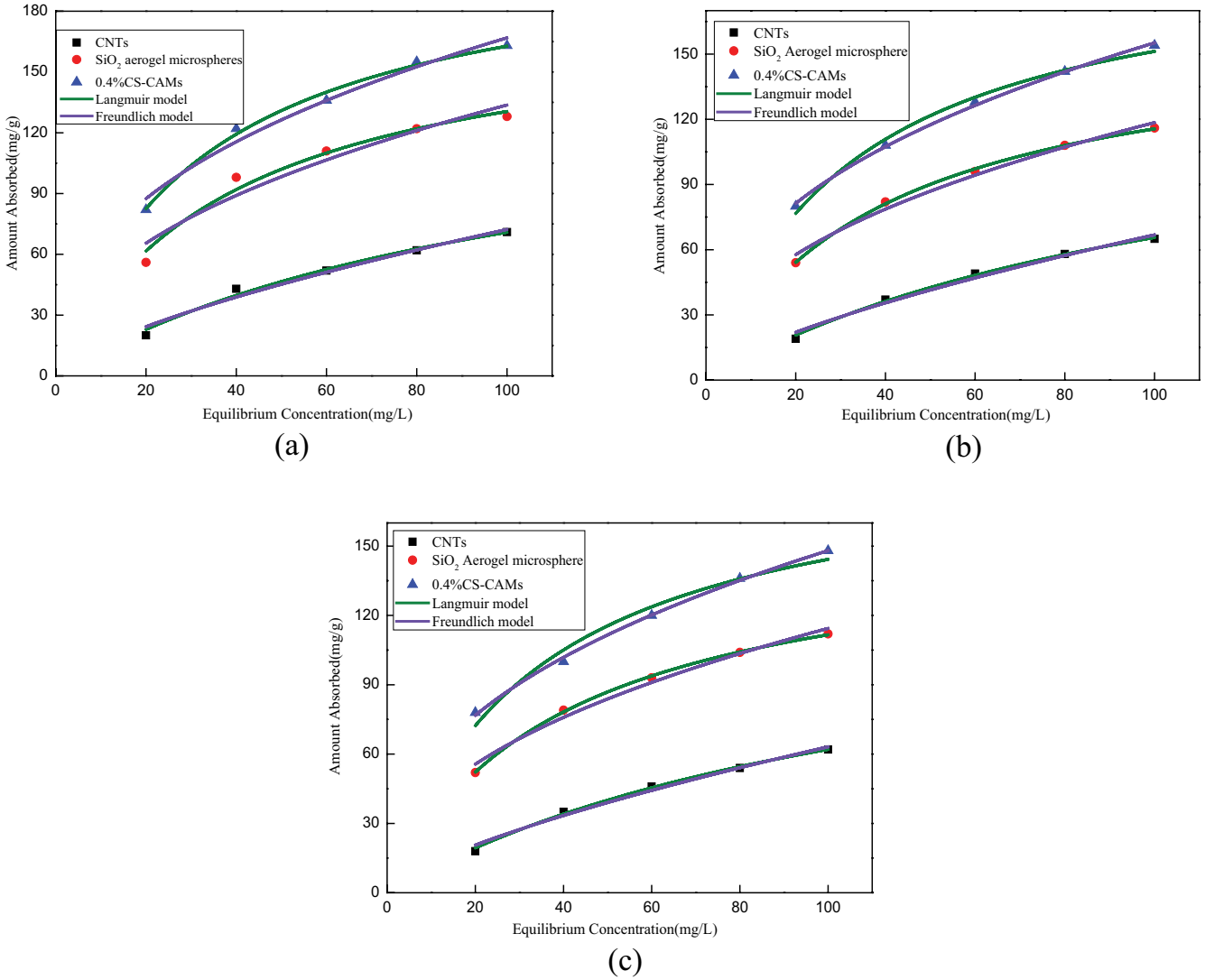

Fig. 10. Adsorption isotherms of toluene and isothermal adsorption models: (a) 293 K, (b) 313 K, and (c) 333 K.

Langmuir model, and the purple solid line represents the data fitted by Freundlich model. The corresponding optimum parameters are listed in Tables 2 and 3. The correlation coefficient (R^2) presented in Table 2 reveal that all the adsorption isotherm curves of toluene can fit both Langmuir equation and Freundlich equation well. For 0.4% CS-CABs, the R^2 of Freundlich equation is larger than that of Langmuir equation, which indicates that its heterogeneous surface adsorption [14] characterizes by progressive adsorption. In addition, the active sites on the surface of the composite

Table 2
Parameters of the Langmuir equation for the adsorption of toluene

Sample	Temperature (K)	$q_e = q_{max}\frac{K_L C_e}{1+K_L C_e}$		
		q_{max} (mg/g)	K_L (L/mg)	R^2
CNTs	293	148.8168	0.0091	0.9826
	313	143.3898	0.0084	0.9953
	333	137.7384	0.0082	0.9959
SiO_2 aerogels beads	293	181.1558	0.0258	0.9694
	313	161.4452	0.0252	0.9986
	333	156.0323	0.0251	0.9991
0.4% CS-CABs	293	214.9526	0.0312	0.9913
	313	199.8931	0.0311	0.9877
	333	192.0581	0.0302	0.9635

Table 3
Parameters of the Freundlich equation for the adsorption of toluene

Sample	Temperature (K)	$\ln q_e = \ln K_F + \frac{1}{n}\ln C_e$		
		K_F (L/mg)	$1/n$	R^2
CNTs	293	3.1961	0.6772	0.9670
	313	2.7825	0.6903	0.9806
	333	2.5724	0.6950	0.9844
SiO_2 aerogels beads	293	17.3342	0.4436	0.9096
	313	15.1108	0.4472	0.9807
	333	14.5299	0.4480	0.9804
0.4% CS-CABs	293	26.2962	0.4012	0.9699
	313	24.3972	0.4018	0.9977
	333	22.5864	0.4083	0.9976

aerogels beads are continuously occupied, and the bonding strength to the adsorbent will gradually reduce, eventually reaching an adsorption equilibrium. The Freundlich exponent $1/n$ between 0.1 and 1 indicates favorable adsorption and a high affinity of 0.4% CS-CABs for toluene. If 'n' is below 1, adsorption is a chemical process, otherwise is a physical process. Thus it is clear that this adsorption is a physical process here [14]. The value of q_m, which is defined as the maximum capacity of adsorbent, has been calculated from the Langmuir plot, and was consistent with the measured one. Such excellent adsorption properties prove that a certain amount of doped CNTs can improve the adsorption performance of aerogels beads. The possible reasons lay on that through the surface modification, CS-CABs exhibited strong hydrophobicity, which was beneficial for binding toluene in aqueous solution. Furthermore, the CNTs and toluene also tend to combine in the form of π–π interaction, which enhances the binding ability of the CS-CABs with toluene. Therefore, the doping of CNTs not only increased the pore size, pore volume and specific surface area of aerogels, but also greatly enhanced the adsorption properties of the materials [6].

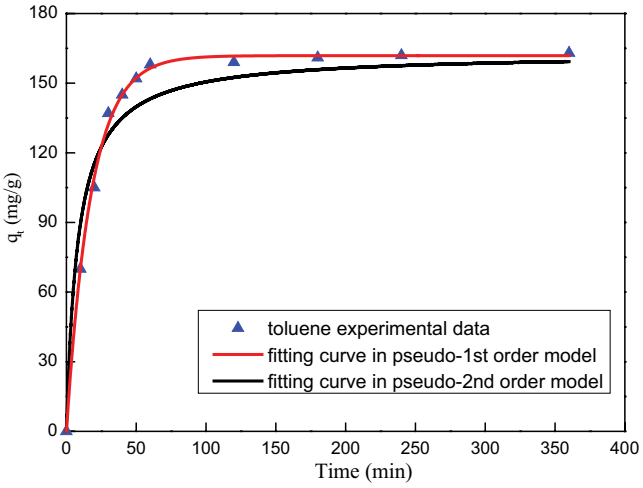

Fig. 11. Pseudo-second-order model.

Table 4
Adsorption kinetics parameters

Adsorbate	Pseudo-first-order dynamics		Pseudo-second-order dynamics	
	K (×10^{-4} min^{-1})	R^2	K (min^{-1})	R^2
Toluene	7.4067	0.9576	0.0565	0.99764

Furthermore, kinetics study on toluene adsorption was carried out, and the classical kinetic models pseudo-first-order [Eq. (4)] and pseudo-second-order [Eq. (5)] models were applied to fit these obtained adsorption processes, which is helpful to determine the nature of adsorption mechanisms and the efficiency of adsorbent in removing pollutants.

The experimental data, kinetic model curves, and equation parameters are provided in Fig. 11 and Table 4. It can be observed from the fitting curves that compared with the pseudo-second-order model, the pseudo-first-order model fitted better with the experiment results, which can also be confirmed by its R^2 value which is closer to 1, indicating that physical-adsorption controls the adsorption of toluene on mesoporous 0.4% CS-CABs materials [46]. In all adsorbent cases, three steps are observed: (a) the first step, where a rapid adsorption appeared within 1 h of contact time; (b) the second-step, where a progressive adsorption occurred thereafter; (c) the adsorbed amount remained constant after about 6 h of contact time, implying the arrival of equilibrium. During the initial adsorption stage, the adsorbent can quickly enter into the internal pores of the material. With the extension of time, the diffusion distance of the adsorbent into the material increases. In addition, the part occupation of active sites cause that the resistance of the diffusion process increases continuously. The two factors mentioned above together contribute to the decline of the adsorbing rate.

4. Conclusion

In summary, we prepared one kind of CNTs/silica composite aerogels beads CS-CABs, with silica sol as precursor and CNTs as dopant, by a W/O emulsion method through a sol–gel process. The results show that the morphology of CS-CABs is influenced by the doping of CNTs: when the doping amount is 0.4%, 0.6% or 0.8%, the CS-CABs show a globule structure with a uniform particle size. While the doping amount is 0.2% or 1%, the sample structure is irregular. When the doping amount is 0.4%, the bulk density, specific surface area, and average pore diameter reach maximum of 320 kg/m^3, 321 m^2/g and 38.56 nm, respectively. The maximum saturated adsorption of 0.4% CS-CAB for toluene in the aqueous solution at 293 K reaches 214 mg/g, which is 1.2 and 1.4 times that of silica aerogels beads and CNTs, respectively. It is attributed to the π–π interactions between the doped CNTs and toluene, the affinity for toluene of the hydrophobic modified functional group, and the large pore size and specific surface area of 0.4% CS-CAB. The adsorption process, which conforms to the Freundlich isothermal adsorption model and the quasi-first-order kinetic model, is mainly physical adsorption.

Declaration of interests

The authors declare that they have no known competing financial interests or personal relationships that could have appeared to influence the work reported in this paper.

Acknowledgement

The work was partial financially supported by National Natural Science Foundation of China (21806122).

References

[1] I. Ihsanullah, M. Sajid, S. Khan, M. Bilal, Aerogel-based adsorbents as emerging materials for the removal of heavy metals from water: progress, challenges, and prospects, Sep. Purif. Technol., 291 (2022) 120923, doi: 10.1016/j.seppur.2022.120923.
[2] R. Ganesamoorthy, V. Kumar Vadivel, K. Rajnish, O.S. Kushwaha, H. Mamane, Aerogels for water treatment: a review, J. Cleaner Prod., 329 (2021) 129713, doi: 10.1016/j.jclepro.2021.129713.
[3] K.-J. Lee, Y.H. Kim, J.K. Lee, H.-J. Hwang, Fast synthesis of spherical silica aerogel powders by emulsion polymerization from water glass, Chemistry Select, 3 (2018) 1257–1261.
[4] A. Lamy-Mendes, W.J. Malfait, A. Sadeghpour, A.V. Girão, R.F. Silva, L. Durães, Influence of 1D and 2D carbon nanostructures in silica-based aerogels, Carbon, 180 (2021) 146–162.
[5] X. Zhou, S. Cui, Y. Liu, X. Liu, X. Shen, Z. Wu, Adsorption capacity of hydrophobic SiO_2 aerogel/activated carbon composite materials for TNT, Sci. China Technol. Sci., 56 (2013) 1767–1772.
[6] R. Tang, W. Hong, C. Srinivasakannan, X. Liu, X. Wang, X. Duan, A novel mesoporous Fe-silica aerogel composite with phenomenal adsorption capacity for malachite green, Sep. Purif. Technol., 281 (2022) 119950, doi: 10.1016/j.seppur.2021.119950.
[7] J. Zhu, J. Xie, X. Lü, D. Jiang, Synthesis and characterization of superhydrophobic silica and silica/titania aerogels by sol–gel method at ambient pressure, Colloids Surf., A, 342 (2009) 97–101.
[8] M. Firoozmandan, J. Moghaddas, N. Yasrebi, Performance of water glass-based silica aerogel for adsorption of phenol from aqueous solution, J. Sol-Gel Sci. Technol., 79 (2016) 67–75.
[9] A. Abbas, B.A. Abussaud, Ihsanullah, N.A.H. Al-Baghli, H.H. Redhwi, Adsorption of toluene and paraxylene from aqueous solution using pure and iron oxide impregnated carbon nanotubes: kinetics and isotherms study, Bioinorg. Chem. Appl., 2017 (2017) 2853925, doi: 10.1155/2017/2853925.
[10] H. Pourzamani, M. Hashemi, B. Bina, A. Rashidi, Toluene removal from aqueous solutions using single-wall carbon nanotube and magnetic nanoparticle–hybrid adsorbent, J. Environ. Eng., 144 (2018) 04017104, doi: 10.1061/(ASCE)EE.1943-7870.0001318.
[11] F. Su, C. Lu, S. Hu, Adsorption of benzene, toluene, ethylbenzene and p-xylene by NaOCl-oxidized carbon nanotubes, Colloids Surf., A, 353 (2010) 83–91.
[12] A. Enright, G. Collins, V. O'Flaherty, Low-temperature anaerobic biological treatment of toluene-containing wastewater, Water Res., 41 (2007) 1465–1472.
[13] C. Ma, R. Ruan, Adsorption of toluene on mesoporous materials from waste solar panel as silica source, Appl. Clay Sci., 80–81 (2013) 196–201.
[14] C. Zhang, C. Dai, H. Zhang, S. Peng, X. Wei, Y. Hu, Regeneration of mesoporous silica aerogel for hydrocarbon adsorption and recovery, Mar. Pollut. Bull., 122 (2017) 129–138.
[15] X. Yan, F. Liu, G. Mu, Z. Zhou, Y. Xie, L. Li, Y. Yang, X. Wang, Adsorption of toluene vapours on micro–meso hierarchical porous carbon, Micro Nano Lett., 13 (2018) 641–645.
[16] F. Liu, X. Yan, F.T. Fan, C.C. Zhao, R.T. Liu, Y. Gao, Y.Q. Wang, Application of micro-meso hierarchical porous carbon for toluene adsorption treatment, Micro Nano Lett., 11 (2016) 372–377.
[17] K.A. Sashkina, P.A. Gurikov, A.B. Ayupova, I. Smirnova, E.V. Parkhomchuk, Zeolite/silica aerogel composite monoliths and microspheres, Microporous Mesoporous Mater., 263 (2018) 106–112.
[18] Y. Yamada, K. Yano, Synthesis of monodispersed supermicroporous/mesoporous silica spheres with diameters in the low submicron range, Microporous Mesoporous Mater., 93 (2006) 190–198.
[19] S. Standeker, Z. Novak, Z. Knez, Adsorption of toxic organic compounds from water with hydrophobic silica aerogels, J. Colloid Interface Sci., 310 (2007) 362–368.
[20] H. Liu, W. Sha, A.T. Cooper, M.H. Fan, Preparation and characterization of a novel silica aerogel as adsorbent for toxic organic compounds, Colloids Surf., A, 347 (2009) 38–44.
[21] T. Kumagai, N. Hirota, K. Sato, K. Namiki, H. Maki, T. Tanabe, Saturable absorption by carbon nanotubes on silica microtoroids, J. Appl. Phys., 123 (2018) 233104, doi: 10.1063/1.5025885.
[22] D. Wang, T. Silbaugh, R. Pfeffer, Y.S. Lin, Removal of emulsified oil from water by inverse fluidization of hydrophobic aerogels, Powder Technol., 203 (2010) 298–309.
[23] M. Zhang, Y. Wu, X. Feng, X. He, L. Chen, Y. Zhang, Fabrication of mesoporous silica-coated CNTs and application in size-selective protein separation, J. Mater. Chem., 20 (2010) 5835–5842.
[24] C. Lu, F. Su, S. Hu, Surface modification of carbon nanotubes for enhancing BTEX adsorption from aqueous solutions, Appl. Surf. Sci., 254 (2008) 7035–7041.
[25] I.K. Jung, J.L. Gurav, U.K.H. Bangi, S. Baek, H.H. Park, Silica xerogel films hybridized with carbon nanotubes by single step sol–gel processing, J. Non-Cryst. Solids, 358 (2012) 550–556.
[26] A. Sedova, G. Bar, O. Goldbart, R. Ron, B. Achrai, I. Kaplan-Ashiri, V. Brumfeld, A. Zak, R. Gvishi, H.D. Wagner, R. Tenne, Reinforcing silica aerogels with tungsten disulfide nanotubes, J. Supercrit. Fluids, 106 (2015) 9–15.
[27] A. Sedova, G. Bar, O. Goldbart, R. Ron, B. Achrai, I. Kaplan-Ashiri, V. Brumfeld, A. Zak, R. Gvishi, H.D. Wagner, R. Tenne, Synthesis and characterization of composite materials "aerogel-MWCNT", J. Sol-Gel Sci. Technol., 84 (2017) 1–9.
[28] A.H. Karim, A.A. Jalil, S. Triwahyono, N.H.N. Kamarudin, A Ripin, Influence of multi-walled carbon nanotubes on

textural and adsorption characteristics of in situ synthesized mesostructured silica, J. Colloid Interface Sci., 421 (2014) 93–102.
[29] M. Liu, L. Gan, Y. Pang, Z.J. Xu, Z.X. Hao, L.W. Chen, Synthesis of titania-silica aerogel-like microspheres by a water-in-oil emulsion method via ambient pressure drying and their photocatalytic properties, Colloids Surf., A, 317 (2008) 490–495.
[30] N. Menshutina, P. Tsygankov, S. Ivanov, Synthesis and properties of silica and alginate hybrid aerogel particles with embedded carbon nanotubes (CNTs) for selective sorption, Materials, 12 (2019) 52, doi: 10.3390/ma12010052.
[31] Y. Yu, D. Guo, J. Fang, Synthesis of silica aerogels microspheres by a two-step acid-base sol–gel reaction with emulsification technique, J. Porous Mater., 22 (2015) 621–628.
[32] L. Yang, Y. Wang, G. Luo, Y. Dai, A new 'pH-induced rapid colloid aggregation' method to prepare micrometer-sized spheres of mesostructured silica in water-in-oil emulsion, Microporous Mesoporous Mater., 94 (2006) 269–276.
[33] K.H. Sun, Y.Y. Mi, H.J. Hwang, Fabrication of spherical silica aerogel granules from water glass by ambient pressure drying, J. Am. Ceram. Soc., 94 (2011) 3198–3201.
[34] M. Alnaief, I. Smirnova, In situ production of spherical aerogel microparticles, J. Supercrit. Fluids, 55 (2011) 1118–1123.
[35] B.A. García-Torres, A. Aguilar-Elguezabal, M. Román-Aguirre, L. Alvarez-Contreras, Synthesis of silica aerogels microspheres prepared by ink jet printing and dried at ambient pressure without surface hydrophobization, Mater. Chem. Phys., 172 (2016) 32–38.
[36] P.B. Sarawade, J.K. Kim, A. Hilonga, H.T. Kim, Production of low- density sodium silicate-based hydrophobic silica aerogel beads by a novel fast gelation process and ambient pressure drying process, Solid State Sci., 12 (2010) 911–918.
[37] P.B. Sarawade, J.K. Kim, A. Hilonga, D.V. Quang, S.J. Jeon, H.T. Kim, Synthesis of sodium silicate-based hydrophilic silica aerogel beads with superior properties: effect of heat-treatment, J. Non-Cryst. Solids, 357 (2011) 2156–2162.
[38] S.D. Bhagat, Y.H. Kim, Y.S. Ahn, J.G. Yeo, Textural properties of ambient pressure dried water-glass based silica aerogel beads: one day synthesis, Microporous Mesoporous Mater., 96 (2006) 237–244.
[39] S. Yun, H. Luo, Y. Gao, Superhydrophobic silica aerogels microspheres from methyltrimethoxysilane: rapid synthesis via ambient pressure drying and excellent absorption properties, RSC Adv., 4 (2013) 4535–4542.
[40] S. Zong, W. Wei, Z. Jiang, Z. Yan, J. Zhu, J. Xie, Characterization and comparison of uniform hydrophilic/hydrophobic transparent silica aerogel beads: skeleton strength and surface modification, RSC Adv., 5 (2015) 55579–55587.
[41] K.J. Lee, Y.H. Kim, J.K. Lee, H.J. Hwang, Fast synthesis of spherical silica aerogel powders by emulsion polymerization from water glass, ChemistrySelect, 3 (2018) 1257–1261.
[42] Q. Chen, H. Wang, L. Sun, Preparation and characterization of silica aerogels microspheres, Materials, 10 (2017) 435, doi: 10.3390/ma10040435.
[43] P.S. Rao, S. Kalyani, K.V.N. Suresh Reddy, A. Krishnaiah, Comparison of biosorption of nickel(II) and copper(II) ions from aqueous solution by *Sphaeroplea* algae and acid treated *Sphaeroplea* algae, Sep. Sci. Technol., 40 (2005) 3149–3165.
[44] K.S.W. Sing, Reporting physisorption data for gas/solid systems with special reference to the determination of surface area and porosity (Recommendations 1984), Pure Appl. Chem., 57 (1985) 603–619.
[45] S. Caldwell, D.W. Johnson, M.P. Didsbury, B.A. Murray, J.J. Wu, S.A. Przyborski, N.R. Cameron, Degradable emulsion-templated scaffolds for tissue engineering from thiolene photopolymerisation, Soft Matter, 8 (2012) 10344–10351.
[46] G.T. Burns, Q. Deng, R. Field, J.R. Hahn, C.W. Lentz, A convenient synthesis of silylated silica xerogels, Chem. Mater., 11 (1999) 1275–1284.
[47] A. Svidrytski, D. Hlushkou, M. Thommes, P.A. Monson, U. Tallarek, Modeling the impact of mesoporous silica microstructures on the adsorption hysteresis loop, J. Phys. Chem. C, 124 (2020) 21646–21655.